



Macroscopic measure of the rate of deformation produced by micro-shear banding

R. B. PEŁCHERSKI (WARSZAWA)

PHYSICAL MODEL of shear strain rate produced by active micro-shear bands in metals is formulated and mathematical idealization of micro-shear bands system by means of the theory of singular surface of order one is proposed. Extension of the known averaging procedure over the representative volume element traversed by a strong discontinuity surface is presented. As a result, the macroscopic measure of velocity gradient produced in the course of elastic-plastic deformation with micro-shear banding is derived. The corresponding macroscopic measures of the rate of deformation and material spin, necessary to formulate constitutive description, are also determined.

1. Introduction

INTEGRATED STUDIES on physics and mechanics of large plastic deformations of metals accounting for micro-shear bands require careful analysis of the averaging procedure and proper setting of the resulting description of the effects of micro-shear bands within the continuum theory of materials. Formulation of a complete theory based on the precise micro-to-macro transition remains an open and challenging question. The aim of the paper is to approach this problem merely from the point of view of the contribution of micro-shear banding to kinematics of finite elastic-plastic deformations of metallic solids. The related macroscopic measures of velocity gradient, rate of deformation and material spin, which are necessary to formulate constitutive equations of elastoplasticity at finite strain, have been determined. The derivation is based on the following novel concepts:

- (i) Mathematical idealization of a system (cluster) of active micro-shear bands as propagating singular surface of order one, having properties of a vortex sheet.
- (ii) Formulation of the physical model, which enables to relate the macroscopic shear strain rate with microstructural features of active micro-shear bands and to identify the jump in velocity across the vortex sheet.
- (iii) Extension of the known averaging procedure by introducing the representative volume element (RVE) traversed by the singular surface of vortex sheet type.

The possibility of modelling of the narrow zone of localization as a surface of strong discontinuity in the velocity field was suggested by THOMAS [1] and applied further by VALANIS [2] and SU [3]. The authors observed that the concentration of dislocation movement on a few slip planes can cause abrupt changes of the velocity field on the micro-scale and may lead to velocity jumps accompanying

plastic deformation in macro-level. The theoretical characterization of a shear band, as a surface of discontinuity, across which the jumps in velocity, stress gradient and temperature are allowed, was considered recently by OLMSTED *et al.* [4] for the one-dimensional problem of unidirectional shearing of a slab, which is used typically in a variety of investigations of the so-called “adiabatic shear bands” formation. The results of this study can be applied to derive in a more rigorous manner the constitutive equations, accounting for micro-shear bands with their characteristic geometric pattern, which were obtained previously under certain simplifying assumptions, [5–7]. Standard symbolic notation is used throughout the paper with tensors denoted by boldface characters.

2. Physical motivation

The results of metallographic observations reveal that in heavily deformed metals or even at small strains, if they are preceded by the change of deformation path, a multiscale hierarchy of shear localization modes progressively replaces the crystallographic multiple slip or twinning. Different terminology is used depending on the level of observation. In our study, the term “micro-shear band” is understood as a long and very thin (of order $0.1\ \mu\text{m}$) sheet-like region of concentrated plastic shear, crossing grain boundaries without deviation and forming a definite pattern in relation to the principal directions of strain. It bears very large shear strains and can lie in a “non-crystallographic” position. The term “non-crystallographic” means that micro-shear bands are usually not parallel to a particular, densely packed crystallographic plane, of conventionally possible active slip system in the crystallites they intersect. This change of deformation mode contributes to the development of strain-induced anisotropy and modifies remarkably the material properties. The experimental information about mechanical behaviour and related structural features is reviewed, e.g. in [6, 8 and 9], where comprehensive lists of references are given. The experimental observations show that micro-shear bands, formed e.g. in rolling, are usually inclined by about $\pm 35^\circ$ to the rolling plane and are orthogonal to the specimen lateral face, although there can be considerable deviations from this value within the 15° to 50° range, cf. [8] and [9].

3. Macroscopic averaging and continuum mechanics description in plasticity of metals

The physical constraint on any continuum mechanics approach to metal plasticity, i.e. the physical dimension of the smallest representative volume element (RVE) of crystalline material for which it is possible to define significant overall measures of stress and strain during plastic deformation, was thoroughly discussed by HILL [10–13] and HAVNER [14–16]. According to [10], p. 8: “... the

dimensions must be large compared with the thickness of the glide packets separating the active glide lamellae (generally of order 10^{-4} cm in many metals at ordinary temperatures). Thus, the linear dimension of the smallest crystal whose behaviour can legitimately be considered from the standpoint of the theory of plasticity is probably of order 10^{-3} cm." On the other hand, HAVNER [14–16] argues that, to an observer who can resolve distances to $1\ \mu\text{m}$, the deformation of crystal grains (with the mean grain diameter of order $100\ \mu\text{m}$) within plastically deformed metal polycrystals is relatively smooth. At such a scale of observation, called microscopic level, one can just distinguish between slip lines on crystal surfaces. This slip lines appear on the submicroscopic level as slip line bundles and slip bands of the order of $0.1\ \mu\text{m}$ width, containing numerous glide lamellae between which amounts of slip as great as 10^3 lattice spacings have occurred. Therefore, the minimum dimension of the RVE in the continuum microscopic description of elastic-plastic deformations of crystalline solids is taken in [14] to be of the order of $1\ \mu\text{m}$, i.e. $> 10^3$ lattice spacings. Consequently, the linear dimension of the RVE corresponding to the macroscopic level is often assumed to be of the order of several millimeters, for moderately fine-grained metals, e.g. in [15] the macro-element is assumed as a polycrystalline unit cube having the unit linear dimension $L_0 \approx 1\ \text{mm}$. This discussion is valid under the general assumption that the dominant mechanism of inelastic behaviour is crystallographic slip. In such a case, the theory describing kinematics and constitutive structure of finite elastic-plastic deformations of crystalline solids is well established and the transition between the microscopic and macroscopic levels is well understood (cf. e.g. HILL [11–13], HAVNER [14–16] and MANDEL [17–18], as well as, HILL and RICE [19], PETRYK [20] and STOLZ [21]). In particular, relations between macro-measures of stress, strain and plastic work are related with the volume averages of their micro-measures. It has also been shown that certain structural features of the constitutive relations, as the normality rule or certain constitutive inequalities, are transmitted upwards through a hierarchy of observational levels unchanged, irrespective of the heterogeneity, no matter what is its origin (cf. HILL [22]).

In the averaging procedure, discussed in [11–20], quasi-static deformation processes with negligible body forces are typically assumed. This means that within the reference volume V_0 of the macroscopic RVE (macro-element), the nominal stress field \mathbf{s}_m , representing micro-stresses, and their rates $\dot{\mathbf{s}}_m$ are self-equilibrated

$$(3.1) \quad \text{Div} \mathbf{s}_m = 0, \quad \text{Div} \dot{\mathbf{s}}_m = 0 \quad \text{in } V_0$$

and with boundary conditions

$$(3.2) \quad \boldsymbol{\nu}_0 \mathbf{s}_m = \mathbf{t}_\nu, \quad \boldsymbol{\nu}_0 \dot{\mathbf{s}}_m = \dot{\mathbf{t}}_\nu \quad \text{on } \partial V_0,$$

where $\boldsymbol{\nu}_0$ is the externally directed unit vector normal to the reference volume at a point on its boundary ∂V_0 . The averaging procedure and micro-to-macro transition, studied within the framework of finite strain theory by HILL [11–13] and

HAVNER [14–16] lead, in particular, to the following relations for the macroscopic measures of the deformation gradient \mathbf{F} and its rate $\dot{\mathbf{F}}$, which are expressed, with use of Gauss' theorem (divergence theorem), by means of the surface data

$$(3.3) \quad \mathbf{F} \equiv \{\mathbf{f}\} = \frac{1}{V_0} \int_{V_0} \text{Grad} \boldsymbol{\chi}_m dV_0 = \frac{1}{V_0} \int_{\partial V_0} \mathbf{x}_m \otimes \boldsymbol{\nu}_0 dA_0,$$

$$(3.4) \quad \dot{\mathbf{F}} \equiv \{\dot{\mathbf{f}}\} = \frac{1}{V_0} \int_{V_0} \text{Grad} \dot{\boldsymbol{\chi}}_m dV_0 = \frac{1}{V_0} \int_{\partial V_0} \dot{\boldsymbol{\chi}}_m \otimes \boldsymbol{\nu}_0 dA_0.$$

Here the symbol $\boldsymbol{\chi}_m$ denotes a microscopic field of motion of the material point \mathbf{X}_m in the reference configuration of the RVE into its current position \mathbf{x}_m

$$(3.5) \quad \mathbf{x}_m = \boldsymbol{\chi}_m(\mathbf{X}_m, t),$$

and the microscopic velocity \mathbf{v}_m is determined in the current configuration

$$(3.6) \quad \mathbf{v}_m = \mathbf{v}_m(\mathbf{x}_m, t) = \mathbf{v}_m(\boldsymbol{\chi}_m(\mathbf{X}_m, t), t) \equiv \dot{\boldsymbol{\chi}}_m(\mathbf{X}_m, t).$$

The Gauss theorem applied above, was specified for any vector field $\mathbf{w} = \mathbf{w}(\mathbf{X}_m)$ defined on the closure $\bar{V}_0 = V_0 \cup \partial V_0$ and being of class $C^0(\bar{V}_0)$ and piecewise of class $C^1(V_0)$, so that \mathbf{w} is continuous on the closure \bar{V}_0 and piecewise continuously differentiable on V_0 (cf. e.g. SMITH [23]). Similarly, the following relations for the macroscopic measures of the suitably smooth tensor field of nominal stress \mathbf{S}

$$(3.7) \quad \mathbf{S} \equiv \{\mathbf{s}_m\} = \frac{1}{V_0} \int_{V_0} \mathbf{s}_m dV_0 = \frac{1}{V_0} \int_{\partial V_0} \mathbf{X} \otimes \mathbf{t}_\nu dA_0,$$

its rate $\dot{\mathbf{S}}$

$$(3.8) \quad \dot{\mathbf{S}} \equiv \{\dot{\mathbf{s}}_m\} = \frac{1}{V_0} \int_{V_0} \dot{\mathbf{s}}_m dV_0 = \frac{1}{V_0} \int_{\partial V_0} \mathbf{X} \otimes \dot{\mathbf{t}}_\nu dA_0$$

and the Kirchhoff stress $\boldsymbol{\tau}$

$$(3.9) \quad \boldsymbol{\tau} \equiv \{\boldsymbol{\tau}_m\} = \{\mathbf{f} \mathbf{s}_m\} = \frac{1}{V_0} \int_{\partial V_0} \mathbf{x} \otimes \mathbf{t}_\nu dA_0$$

can be obtained by application of Gauss' theorem and (3.1), cf. [11].

4. Basic kinematical relations

In plasticity of single crystals, it is usually assumed that dislocations traversing a volume element produce a change of its shape, but they do not change its lattice orientation. This leads to the fundamental assumption in elastoplasticity models for metals, which says that distinction should be made between kinematics of the continuum and kinematics of the underlying crystallographic structure. The macroscopic counterpart of such a situation in finite deformation plasticity of polycrystals is Mandel's concept of the intermediate, relaxed, configuration, called isoclinic one, in which the chosen director triad preserves always the same orientation with respect to the fixed axes of the laboratory reference frame. In such a case, we can understand that the director vectors are introduced as a tool to monitor at any instant the state of the strain-induced anisotropy. Different visualizations of such a triad are discussed e.g. in [17], and [24–29], where more detailed discussion and further references can be found. The assumption that the continuum is endowed with the structure in the form of the director vectors leads to the concepts of the local, relaxed, intermediate isoclinic configurations, plastic spin and structure corotational rate. Due to this, the decomposition of the deformation gradient \mathbf{F} becomes unique, [17]

$$(4.1) \quad \mathbf{F} = \mathbf{E} \mathbf{P},$$

where \mathbf{E} denotes the elastic transformation from the intermediate isoclinic configuration to the current one, and \mathbf{P} is the plastic transformation from the reference configuration to the isoclinic one. The following basic kinematical relations hold:

$$(4.2) \quad \mathbf{L} = \dot{\mathbf{E}}\mathbf{E}^{-1} + \mathbf{E}\dot{\mathbf{P}}\mathbf{P}^{-1}\mathbf{E}^{-1}, \quad \mathbf{L} = \mathbf{D} + \mathbf{W},$$

$$(4.3) \quad \mathbf{D} = \mathbf{D}^e + \mathbf{D}^p, \quad \mathbf{W} = \mathbf{W}^e + \mathbf{W}^p,$$

$$(4.4) \quad \mathbf{D}^e = \{\dot{\mathbf{E}}\mathbf{E}^{-1}\}_s, \quad \mathbf{D}^p = \{\mathbf{E}\dot{\mathbf{P}}\mathbf{P}^{-1}\mathbf{E}^{-1}\}_s,$$

$$(4.5) \quad \mathbf{W}^e = \{\dot{\mathbf{E}}\mathbf{E}^{-1}\}_a, \quad \mathbf{W}^p = \{\mathbf{E}\dot{\mathbf{P}}\mathbf{P}^{-1}\mathbf{E}^{-1}\}_a,$$

where $\mathbf{L} = \dot{\mathbf{F}}\mathbf{F}^{-1}$ is the velocity gradient, \mathbf{D} and \mathbf{W} correspond to the rate of deformation and material spin, respectively, and the superscripts e and p refer to elastic and plastic states, whereas the symbols $\{\mathbf{t}\}_s$ and $\{\mathbf{t}\}_a$ denote the symmetric and skew-symmetric parts of the second-order tensor \mathbf{t} . A similar decomposition, such as in (4.1), was proposed earlier by LEE [30] within the context of finite elastic-plastic deformation of continuous body, without explicit definition of a structure or director vectors and isoclinic configuration. Such an approach is completely different from that presented above and can be considered as an alternative to the plasticity theory of structured solids.

5. Physical model of shear strain rate produced by active micro-shear bands

Consider certain RVE containing the region of progressive shear banding, depicted schematically in Fig. 1 a, where the traces of successive clusters of micro-shear bands are shown. The arrow points to the direction of expansion of the region. According to the results of experimental observations presented in [8–9] and [31], an active shear band consists of the clusters of micro-shear bands of

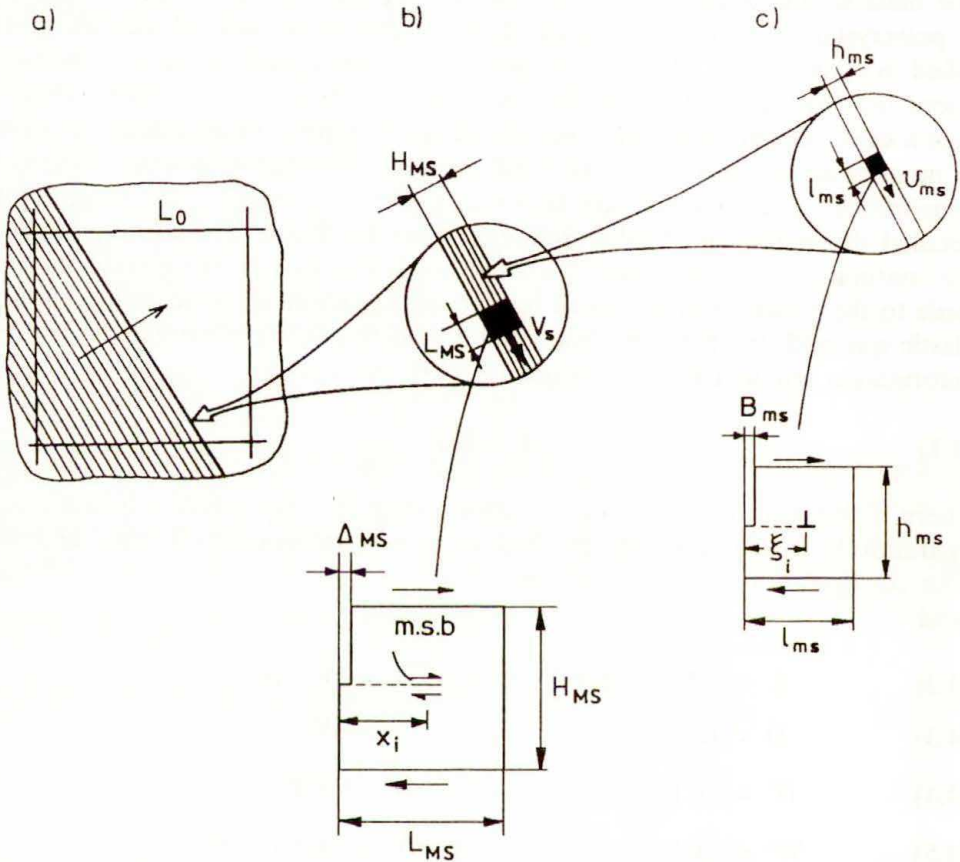


FIG. 1. Schematic illustration of the multiscale, hierarchically organized system of shear banding: a) The section of the unit cube of the RVE, having the dimension $L_0 \approx 1$ mm, traversed by the region of shear banding progressing in the direction pointed by the arrow. b) The cluster of active micro-shear bands with the active zone of the thickness $H_{MS} \approx (10 \div 100) \mu\text{m}$ and the width L_{MS} being of the same order. Beneath, the fundamental mechanism of plastic shear strain generated by the active micro-shear bands (m.s.b.), which operate within the active zone, moving along the distances x_i , $i = 1, 2, 3, \dots, N_{MS}$, during their “lifetime”, and produce the total displacement Δ_{MS} of the top of the active zone relative to the bottom, is depicted. c) The active zone of a single micro-shear band of the thickness $h_{ms} \approx 0.1 \mu\text{m}$ and the width l_{ms} of the same order. Below, the picture of an elementary dislocation model of plastic shear in the active zone is shown. The displacement B_{ms} of the top of the active zone with respect to the bottom is produced by n dislocations moving at the distances ξ_i , $i = 1, 2, 3, \dots, n$.

the thickness of order $(10 \div 100) \mu\text{m}$, which at this level of observation can be considered as elementary carriers of plastic strain. On the other hand, an active micro-shear band is produced as the effect of spatial and time organization of large number of dislocations, which generate and move collectively within a long and thin sheet-like regions, crossing grain boundaries without deviation and having the thickness of order $0.1 \mu\text{m}$. Therefore, from the point of view of kinematics, the micro-shear band can be considered as a thin region of concentrated plastic shear. During the passage of the active zone, of thickness h_{ms} and width l_{ms} , the local perturbation, B_{ms} , of the microscopic displacement field is produced which travels at the head of the micro-shear band with the speed v_{ms} as a distortion wave, cf. Fig. 1 c. According to [31], l_{ms} can be interpreted as the mean diameter of the dislocation islands observed on TEM micrographs. Therefore, one can assume that approximately $l_{ms} \approx h_{ms}$. According to the discussion in [32], the width l_{ms} corresponds also to the dimension of the range of stress pulse produced by dynamic pile-up of a group of dislocations, which is necessary for the transmission process through the grain boundary and activation of a micro-shear band. In Fig. 1, two successive “magnifications” of the shear banding area are “zoomed in” and the related fundamental mechanisms of plastic shear are illustrated. The first one, depicted in Fig. 1 b, corresponds to the cluster of micro-shear bands, having the active zone of thickness H_{MS} and the width L_{MS} , in which the passage of large number of active micro-shear bands results in the local perturbation, Δ_{MS} , of the microscopic displacement field $\mathbf{u}_m = \mathbf{x}_m - \mathbf{X}_m$, which moves with the speed V_s . The second “magnification”, shown in Fig. 1 c, represents the aforementioned active zone of a single micro-shear band.

Consider an elementary dislocation model of plastic shear produced in the active zone at the head of a single micro-shear band, as it is depicted in Fig. 1 c. According to the known approach, the shear strain results from the generation and movement of large number of dislocations through the active zone, (cf. GILMAN [33] and DIETER [34]), and the following relations hold

$$(5.1) \quad \delta_i = \frac{\xi_i b}{l_{ms}}, \quad B_{ms} = \sum_i^n \delta_i = \frac{b}{l_{ms}} \sum_i^n \xi_i,$$

where δ_i is the displacement of the i -th dislocation at an intermediate position between $\xi_i = 0$ and $\xi_i = l_{ms}$, whereas B_{ms} corresponds, according to Fig. 1 c, to the displacement of the top of the active zone relative to the bottom for n dislocations. The corresponding shear strain γ reads

$$(5.2) \quad \gamma = \frac{B_{ms}}{h_{ms}} = \frac{b n}{l_{ms} h_{ms}} \bar{\xi}, \quad \bar{\xi} = \frac{\sum_i^n \xi_i}{n},$$

where $\bar{\xi}$ is the average distance that dislocations have moved. Assuming that the distance $\bar{\xi}$ and the number of dislocations n can change with the variable τ ,

corresponding to the duration of the microscopic process of plastic shear, the pertinent shear strain rate can be calculated

$$(5.3) \quad \frac{d\gamma}{d\tau} = \frac{b}{l_{ms}h_{ms}} \left(n v_d + \bar{\xi} \frac{dn}{d\tau} \right),$$

where

$$(5.4) \quad v_d = \frac{d\bar{\xi}}{d\tau}$$

is the average dislocation velocity. Finally, the shear strain rate, produced in a singular micro-shear band, can be expressed in terms of the speed v_{ms} of the head of micro-shear band

$$(5.5) \quad \frac{d\gamma}{d\tau} = \frac{v_{ms}}{h_{ms}}, \quad v_{ms} = \frac{b}{l_{ms}} \left(n v_d + \bar{\xi} \frac{dn}{d\tau} \right).$$

According to (5.3), generation and movement of new dislocations contribute to the plastic strain rate. If we assume that the movement of a constant number of mobile dislocations plays the prevalent role, (5.3) transforms into the well known Orowan relation

$$(5.6) \quad \frac{d\gamma}{d\tau} = b \varrho v_d, \quad \varrho = \frac{n}{l_{ms}h_{ms}},$$

where ϱ denotes the dislocation density. In the case of micro-shear bands propagation, the systems which are not necessarily parallel to densely packed crystallographic planes are activated. The critical stress in such planes is very high and therefore, the generation of new dislocations may contribute remarkably to plastic shear strain rate. In such a case relation (5.5) seems to be justified. It is, however, difficult to follow experimentally the interplay of both the mechanisms of generation and movement of dislocations to provide a unique assessment of their contribution to the plastic strain rate (cf. e.g. KORBEL [35]).

Consider a certain number of active micro-shear bands N_{MS} of similar orientation and produced within certain time period, $\bar{\tau} = \tau_f - \tau_i$, which can be considered as an infinitesimal increment, Δt , of "time-like parameter" in the macroscopic description. As it is depicted schematically in Fig. 1 b, such a system (cluster) of micro-shear bands produces the microscopic shear strain γ_{ms} , which is given by the following relation

$$(5.7) \quad \gamma_{ms} = \frac{\Delta_{MS}}{H_{MS}}, \quad \Delta_{MS} = \frac{\bar{B}_{ms} N_{MS}}{L_{MS}} \bar{x}_{MS},$$

where \bar{B}_{ms} is the total displacement produced by a single micro-shear band

$$(5.8) \quad \bar{B}_{ms} = h_{ms} \bar{\gamma} = \int_{\tau_i}^{\tau_f} v_{ms} d\tau,$$

and

$$(5.9) \quad \bar{x}_{MS} = \frac{\sum_i^n x_i}{n}, \quad n \equiv N_{MS},$$

denotes the average distance that N_{MS} micro-shear bands have moved, during their “lifetime”, in the active zone. Assuming that the distance \bar{x}_{MS} and the number of active micro-shear bands N_{MS} can change during propagation of the active zone of the cluster, we have from (5.7)

$$(5.10) \quad \dot{\gamma}_{ms} = \frac{\bar{B}_{ms}}{L_{MS}H_{MS}} \left(N_{MS}\dot{\bar{x}}_{MS} + \bar{x}_{MS}\dot{N}_{MS} \right),$$

where the dot denotes differentiation with respect to the “time-like parameter” t . Let us observe that the rate $\dot{\bar{x}}_{MS}$ can be identified with the speed v_{ms} of the head of a single micro-shear band, $\dot{\bar{x}}_{MS} \equiv v_{ms}$, under the simplifying assumption that v_{ms} is approximately the same for each micro-shear band in the active zone of the cluster. Then, the speed of propagation of the disturbance of the microscopic displacement field, V_S , produced in the active zone of the cluster of N_{MS} active micro-shear bands, is given by

$$(5.11) \quad V_S = \frac{\bar{B}_{ms}}{L_{MS}} \left(N_{MS}v_{ms} + \bar{x}_{MS}\dot{N}_{MS} \right),$$

and the shear strain rate reads

$$(5.12) \quad \dot{\gamma}_{ms} = \frac{V_S}{H_{MS}}.$$

If the number of active micro-shear bands in the active zone can be assumed constant, the relation for the speed V_S is given by

$$(5.13) \quad V_S = \frac{\bar{B}_{ms}}{L_{MS}} N_{MS}v_{ms}$$

and (5.12) takes the form, which is formally similar to the Orowan relation (5.6)

$$(5.14) \quad \dot{\gamma}_{ms} = \bar{B}_{ms}\varrho_{MS}v_{ms}, \quad \varrho_{MS} = \frac{N_{MS}}{L_{MS}H_{MS}},$$

where ϱ_{MS} corresponds to the active micro-shear bands density. It is a matter of further investigations upon the evolution of clusters of micro-shear bands to confirm the usefulness of this hypothesis.

The experimental observations and certain analogy with martensitic transformations, lead to the hypothesis that micro-shear bands propagate with the velocity v_{ms} of constant value, which is close to the shear wave speed c_s (velocity of sound) in the considered metal or alloy. Thus, the following relation is physically justified

$$(5.15) \quad v_{ms} = \eta c_s = \eta \left(\frac{\mu}{\rho} \right)^{1/2}, \quad \eta \in (0, 1),$$

where η corresponds to the factor accounting for the effect of dissipation related with nucleation and movement of dislocations in the activated systems. The value of η can be determined, at least theoretically, from (5.5)₂. However, it is difficult to evaluate experimentally, in a consistent way, all the structural parameters occurring in (5.5)₂. Therefore, the direct measurements of v_{ms} seem to be more appropriate. For instance, the results of shear band speed measurements in C – 300 steel (a high strength maraging steel) have been reported recently by ZHOU *et al.* [36]. The highest speed observed is close to 1200 ms⁻¹, i.e. approximately 40% of the shear wave speed c_s of the specimen material. This gives the estimate of $\eta \approx 0.40$. The investigated shear bands correspond to the clusters of micro-shear bands. According to (5.13), the speed of a single micro-shear band should be much higher, what will produce also higher value of η . The complementary evaluation of structural parameters, \bar{B}_{ms} , L_{MS} and N_{MS} , of the investigated shear bands is necessary to obtain more exact specification of η .

6. System of active micro-shear bands as a surface of strong discontinuity

The foregoing discussion of physical nature of micro-shear banding process, as well as the recent results of the microscopic observations *in situ*, presented by YANG and REY [37] and REY *et al.* [38], support the following hypothesis:

The passage of micro-shear bands within the active zone of the cluster, results in the perturbation of the microscopic displacement field travelling with the speed V_s , which produces a discontinuity of the microscopic velocity field in the RVE it traverses. The progression of clusters of micro-shear bands can be idealized mathematically by means of a singular surface of order one propagating through the macro-element (RVE) of the continuum.

The necessary mathematical formalism of the theory of propagating singular surfaces is given, e.g. by TRUESDELL and TOUPIN [39], ERINGEN and SUHUBI [40] and KOSIŃSKI [41]. The theory allows to identify the postulated discontinuity surface of the microscopic velocity field \mathbf{v}_m in RVE as a singular surface $\Sigma(t)$ moving in the region V_0 of the reference configuration of the body, where for each instant of “time-like parameter” $t \in I \subset \mathbb{R}$, the surface $\Sigma(t) \subset V_0$ has the dual counterpart $S(t) \subset V$, in the spatial configuration. There exists the jump

discontinuity of derivatives of the function of motion χ_m , i.e. of the microscopic velocity field $[\dot{\chi}_m] \neq \mathbf{0}$ and the deformation gradient $[\mathbf{f}] \neq \mathbf{0}$, which are assumed to be smooth in each point of $V_0 \times I$ outside the discontinuity surface:

$$(6.1) \quad [[\dot{\chi}_m]] = \dot{\chi}_m^+ - \dot{\chi}_m^- \neq 0, \quad [[\mathbf{f}]] = \mathbf{f}^+ - \mathbf{f}^- \neq 0.$$

According to [39] and [41], the considered surface of strong discontinuity of microscopic velocity field fulfills the properties of a vortex sheet with the jump discontinuity of the first derivatives of χ_m given by

$$(6.2) \quad [[\mathbf{v}]] = V_S \mathbf{s}, \quad [[\mathbf{f}]] = -\frac{V_S}{U} \mathbf{s} \otimes \mathbf{n} \mathbf{f}, \quad \text{for } U \neq 0,$$

where \mathbf{s} and \mathbf{n} are, respectively, the unit tangent and the unit normal vectors to the discontinuity surface $S(t)$, while U corresponds to the local intrinsic speed of propagation of $S(t)$, (cf. [39], p.508). Similarly, for the material counterpart of a singular surface $\Sigma(t)$, the compatibility relations take the form

$$(6.3) \quad [[\dot{\chi}_m]] = V_S \mathbf{s}, \quad [[\mathbf{f}]] = -\frac{V_S}{U_N} \mathbf{s} \otimes \mathbf{N} \quad \text{for } U_N \neq 0,$$

where \mathbf{N} is the unit vector normal to the discontinuity surface $\Sigma(t)$ and U_N is the normal component of the surface velocity (cf. [40], p.96).

7. Problem of macroscopic averaging and continuum mechanics description of micro-shear banding

Application of the generalized form of Gauss' theorem for the gradient of the microscopic velocity field $\dot{\chi}_m$, which is sufficiently smooth in each point of $V_0 \times I$ except the singular surface, where the discussed jump discontinuity $[[\dot{\chi}_m]]$ appears, leads to (cf. e.g. [41], p.68 or [42], p.427)

$$(7.1) \quad \int_{V_0} \text{Grad} \dot{\chi}_m dV_0 = \int_{\partial V_0 - \Sigma(t)} \dot{\chi}_m \otimes \boldsymbol{\nu}_0 dA_0 - \int_{\Sigma(t)} [[\dot{\chi}_m]] \otimes \mathbf{N} dA_0.$$

Due to (7.1), the averaging procedure (3.4) of the microscopic velocity field $\dot{\chi}_m$ over the macro-element V_0 can be generalized to the macroscopic RVE traversed by a singular surface of order one. The macroscopic measure of the deformation gradient \mathbf{F} and its rate $\dot{\mathbf{F}}$ are expressed by means of surface data in the following way

$$(7.2) \quad \mathbf{F} \equiv \frac{1}{V_0} \int_{\partial V_0 - \Sigma(t)} \mathbf{x}_m \otimes \boldsymbol{\nu}_0 dA_0,$$

where according to (3.3) $\mathbf{F} = \mathbf{F}$, and

$$(7.3) \quad \dot{\mathbf{F}} \equiv \frac{1}{V_0} \int_{\partial V_0 - \Sigma(t)} \boldsymbol{\chi}_m \otimes \mathbf{v}_0 dA_0 = \frac{1}{V_0} \int_{V_0} \text{Grad} \dot{\boldsymbol{\chi}}_m dV_0 + \frac{1}{V_0} \int_{\Sigma(t)} [[\dot{\boldsymbol{\chi}}_m]] \otimes \mathbf{N} dA_0.$$

Similarly, application of the generalized form of Gauss' theorem for the stress field \mathbf{s}_m over the macro-element V_0 with the singular surface, gives the formula for the average nominal stress

$$(7.4) \quad \mathbf{F} \equiv \frac{1}{V_0} \int_{\partial V_0 - \Sigma(t)} \mathbf{X}_m \otimes \mathbf{t}_\nu dA_0 = \frac{1}{V_0} \int_{V_0} \mathbf{s}_m dV_0 + \frac{1}{V_0} \int_{\Sigma(t)} \boldsymbol{\xi} \otimes [[\mathbf{t}_N]] dA_0,$$

where

$$(7.5) \quad \mathbf{t}_N = \mathbf{N} \mathbf{s}_m(\boldsymbol{\xi}), \quad \boldsymbol{\xi} \in \Sigma(t).$$

The dynamical compatibility condition for the jump of the tractions $[[\mathbf{t}_N]]$ across the singular surface in the reference configuration $\Sigma(t)$ takes the form (cf. e.g. [40], p. 34)

$$(7.6) \quad \mathbf{N}[[\mathbf{s}_m]] = -\rho U_N [[\dot{\boldsymbol{\chi}}_m]].$$

Let us consider the processes in which the jump of inertia forces across the singular surface is negligible. This corresponds to the situation, in which the movement of the singular surface, being the mathematical idealization of the progressing shear banding zone, is approximated by a quasi-static process. In such a case $U_N = 0$ and the jump in the tractions, $[[\mathbf{t}_N]]$, must vanish to ensure the equilibrium condition, what results in vanishing of the integral over $\Sigma(t)$ in (7.4) and restores the classical averaging formula (3.7) (cf. NEMAT-NASSER and HORI [43], p. 37).

Assuming that the singular surface of order one has the properties of the vortex sheet with the velocity jump of magnitude V_S , and accounting in (7.3) for (6.3)₁, we obtain

$$(7.8) \quad \dot{\mathbf{F}} = \frac{1}{V_0} \int_{V_0} \text{Grad} \dot{\boldsymbol{\chi}}_m dV_0 + \frac{1}{V_0} \int_{\Sigma(t)} V_S \mathbf{s} \otimes \mathbf{N} dA_0.$$

If we choose the current configuration of RVE, at time t , as the reference one, the rate of deformation gradient $\dot{\mathbf{F}}$ becomes then the rate of relative deformation

gradient, $\dot{\mathbf{F}}_{(t)}(t)$, at time t (cf. [44], p.54) and the averaging formula (7.8) will take the following spatial form:

$$(7.9) \quad \mathbf{L} \equiv \frac{1}{V} \int_{\partial V-S(t)} \mathbf{v}_m \otimes \boldsymbol{\nu} dA = \frac{1}{V} \int_V \text{grad } \mathbf{v}_m dV + \frac{1}{V} \int_{S(t)} V_S \mathbf{s} \otimes \mathbf{n} dA,$$

where \mathbf{L} denotes the macroscopic measure of velocity gradient $\mathbf{L} \equiv \dot{\mathbf{F}}_{(t)}(t) = \dot{\mathbf{F}}(t)\mathbf{F}^{-1}(t)$, averaged over the macro-element V traversed by the vortex sheet $S(t)$.

The averaging formula (7.9) enables us to account for the contribution of micro-shear banding in the macroscopic measure of velocity gradient produced at finite elastic-plastic strain. According to (7.9), the velocity gradient \mathbf{L} is decomposed as follows:

$$(7.10) \quad \mathbf{L} = \mathbf{L} + \mathbf{L}_{MS}, \quad \mathbf{L}_{MS} = \frac{1}{V} \int_{S(t)} V_S \mathbf{s} \otimes \mathbf{n} dA.$$

Assuming that the singular surface $S(t)$ forms a plane traversing volume V , with the unit vectors \mathbf{s} and \mathbf{n} held constant, (7.10)₂ results in

$$(7.11) \quad \mathbf{L}_{MS} = \dot{\gamma}_{MS} \mathbf{s} \otimes \mathbf{n},$$

where the macroscopic shear strain rate $\dot{\gamma}_{MS}$ is determined, according to (5.11) and (5.12), by the microscopic variables as an average over the RVE

$$(7.12) \quad \dot{\gamma}_{MS} = \frac{1}{V} \int_{S(t)} H_{MS} \dot{\gamma}_{ms} dA = \frac{1}{V} \int_{S(t)} \frac{B_{ms}}{L_{MS}} \left(N_{MS} v_{ms} + \bar{x}_{MS} \dot{N}_{MS} \right) dA.$$

Further experimental and theoretical studies are necessary to identify the structural variables appearing in (7.12) and to prepare more workable formula for the macroscopic shear strain rate produced by micro-shear banding. For instance, the following simplification could be verified. Consider the situation, when the number of the micro-shear bands N_{MS} operating in the active zone does not change much during the deformation process. Then, according to (5.14) and (5.15), the relation (7.12) takes the form

$$(7.13) \quad \dot{\gamma}_{MS} = \frac{1}{V} \int_{S(t)} H_{MS} \dot{\gamma}_{ms} dA = \frac{\eta c_s}{V} \int_{S(t)} H_{MS} B_{ms} \varrho_{MS} dA.$$

For the RVE being the unit cube of the dimension L_0 , (7.13) reads

$$(7.14) \quad \dot{\gamma}_{MS} = \eta \frac{B_{ms} N_{MS}}{L_0 L_{MS}} c_s = \eta \frac{B_{ms}}{n_{SB} D_{SB} d_{MS}} c_s,$$

where n_{SB} is the number of the clusters of micro-shear bands in the RVE, and D_{SB} is the mean distance between them, so that $L_0 = n_{SB}D_{SB}$, while d_{MS} is the mean distance between micro-shear bands in the cluster of the thickness $H_{MS} = N_{MS}d_{MS}$, under the assumption that $L_{MS} \approx H_{MS}$ (cf. Fig. 1).

The derived relations (7.12)–(7.14) are valid for a single system of micro-shear bands. This can be generalized for the case of a double shearing system

$$(7.15) \quad \mathbf{L} = \mathbf{L}_1 + \sum_{i=1}^2 \dot{\gamma}_{MS}^{(i)} \mathbf{s}^{(i)} \otimes \mathbf{n}^{(i)},$$

where $\dot{\gamma}_{MS}^{(i)}$ is the macroscopic shear strain rate and $\mathbf{s}^{(i)}$, $\mathbf{n}^{(i)}$ are the respective unit vectors of the i -th shearing system. It is worthy to note, that (7.15) is valid under the assumption that the active micro-shear bands in both systems operate in the time period, which can be considered as an infinitesimal increment of “time-like parameter” in the macroscopic description. Otherwise, the sequence of events should be taken into considerations. The above relations provide the following macroscopic measures of the rate of plastic deformations and plastic spin produced by active micro-shear bands

$$(7.16) \quad \mathbf{D}_{MS}^p = \frac{1}{2}(\mathbf{L}_{MS} + \mathbf{L}_{MS}^T), \quad \mathbf{W}_{MS}^p = \frac{1}{2}(\mathbf{L}_{MS} - \mathbf{L}_{MS}^T).$$

The discussed averaging procedure over the RVE with the singular surface allows us to account for the characteristic geometric pattern of micro-shear bands which is transmitted upwards through a multiscale hierarchy of observational levels.

8. Concluding remarks

To capture the gross effects of active micro-shear bands, the simplified approach based on the mode of plane deformation of rigid-plastic solid was applied in [5–6]. The contribution of the mechanism of crystallographic multiple slip was approximated by the classical J_2 flow law and the contribution of active micro-shear bands was idealized by means of an additional double-shearing system. This resulted in the additive composition of the rates of plastic deformations as a combination of two modes of pure shear in the plane of plastic flow. The assessment of possible incorporation of the rate equations of plastic flow into an elastic-plastic material model was discussed in [6] and [7]. The approximate description of infinitesimally small elastic strains and large plastic deformations accounting for macroscopic effects of micro-shear banding was proposed in [45–47]. The derivation of the macroscopic measure of the velocity gradient \mathbf{L} given in (7.9) and its additive decomposition (7.10)₁ makes it possible to formulate in a more rigorous manner the constitutive equations of elastoplasticity with

an account of micro-shear banding. Due to (4.1)–(4.3), (7.10)₁ and (7.16), the following kinematical relations hold

$$(8.1) \quad \begin{aligned} \mathbf{D} &= \mathbf{D}^e + \mathbf{D}^p = \mathbf{D}^e + \mathbf{D}_S^p + \mathbf{D}_{MS}^p, \\ \mathbf{W} &= \mathbf{W}^e + \mathbf{W}^p = \mathbf{W}^e + \mathbf{W}_S^p + \mathbf{W}_{MS}^p, \end{aligned}$$

where \mathbf{D}_S^p and \mathbf{W}_S^p correspond, respectively, to the rate of plastic deformation and plastic spin produced by crystallographic multiple slip. The application of the aforementioned relations for constitutive modelling of elastic-plastic behaviour of metallic solids is presented in [47].

This work is focused mainly on the question how the effects of characteristic geometric pattern of micro-shear bands can be transmitted to the macroscopic level and included into the kinematics of finite elasto-plastic strains. Nevertheless, the kinetics of micro-shear banding phenomena with the related dynamic conditions on the strong discontinuity surface (7.6) and the pertinent micro-to-macro transition analysis is also very important. The results obtained by RANIECKI and TANAKA [48] within the context of continuum mechanics description of martensitic phase transformations, with use of the concepts of a surface of strong discontinuity and thermodynamical driving force, provide useful analogies. Further studies are necessary to shed more light on these problems. In particular, the possibility of application of the idea of thermodynamical driving force for the formulation of the criterion of micro-shear band formation deserves further examining.

A fundamental role in the rigorous analysis of the linkages between basic properties at two levels of description of elastic-plastic solids plays the theorem of product averages, which was studied in a general form by HILL [13]. The comprehensive bibliography of earlier papers, confined to small strains, is discussed in the work of NEMAT-NASSER and HORI [44]. The problem of extension of this theorem to the RVE, which is traversed by a propagating strong discontinuity surface, requires further studies.

Acknowledgment

This work was supported by the Committee for Research (KBN) Poland, under the project No. 7 T07A 017 08. The author is indebted to Prof. W. KOSIŃSKI for his critical comments after reading of the manuscript. Also discussions with Prof. H. PETRYK, in particular on the physical model and the averaging procedure, are greatly appreciated.

References

1. T.Y. THOMAS, *Plastic flow and fracture in solids*, Academic Press, New York and London 1961.
2. K.C. VALANIS, *Banding and stability in plastic materials*, *Acta Mech.*, **79**, 113–141, 1989.
3. X.M. SU, *Localized banding with strong velocity jumps*, *Arch. Appl. Mech.*, **62**, 172–180, 1992.

4. W.E. OLMSTEAD, S. NEMAT-NASSER and L. NI, *Shear bands as surfaces of discontinuity*, J. Mech. Phys. Solids, **42**, 697–709, 1994.
5. R.B. PEÇHERSKI, *Physical and theoretical aspects of large plastic deformations involving shear banding*, [in]: Finite Inelastic Deformations. Theory and Applications, Proc. IUTAM Symposium Hannover, Germany 1991, D. BESDO and E. STEIN [Eds.], Springer Verlag, 167–178, 1992.
6. R.B. PEÇHERSKI, *Modelling of large plastic deformations based on the mechanism of micro-shear banding. Physical foundations and theoretical description in plane strain*, Arch. Mech., **44**, 563–584, 1992.
7. R.B. PEÇHERSKI, *Theoretical description of plastic flow accounting for micro-shear bands*, Arch. Metall., **38**, 205–219, 1993.
8. A. KORBEL, *Mechanical instability of metal substructure – catastrophic flow in single and polycrystals*, [in]: Z.S. Basinski International Symposium on Crystal Plasticity, D.S. WILKINSON and J.D. EMBURY [Eds.], Canadian Institute of Mining and Metallurgy, 42–86, 1992.
9. M. HATHERLY and A.S. MALIN, *Shear bands in deformed metals*, Scripta Metall., **18**, 449–454, 1984.
10. R. HILL, *The mechanics of quasi-static plastic deformation in metals*, [in]: Surveys in Mechanics, G.K. BATCHELOR, R.M. DAVIES [Eds.], Cambridge, 7–31, 1956.
11. R. HILL, *On constitutive macro-variables for heterogeneous solids at finite strain*, Proc. Roy. Soc. Lond., **A326**, 131–147, 1972.
12. R. HILL, *On the micro-to-macro transition in constitutive analyses of elastoplastic reponse at finite strain*, Math. Proc. Camb. Phil. Soc., **95**, 481–494, 1984.
13. R. HILL, *On macroscopic effects of heterogeneity in elastoplastic media at finite strain*, Math. Proc. Camb. Phil. Soc., **98**, 579–590, 1985.
14. K.S. HAVNER, *On the mechanics of crystalline solids*, J. Mech. Phys. Solids, **21**, 383–394, 1973.
15. K.S. HAVNER, *Aspects of theoretical plasticity at finite deformation and large pressure*, ZAMP, **25**, 765–781, 1974.
16. K.S. HAVNER, *Finite plastic deformation of crystalline solids*, Cambridge University Press, Cambridge, U.K. 1992.
17. J. MANDEL, *Plasticité classique et viscoplasticité*, C.I.S.M., Springer Verlag, Udine 1972.
18. J. MANDEL, *Mécanique des solides anélastiques. – Généralisation dans R⁹ de la règle du potentiel plastique pour un élément polycristallin*, C. R. Acad. Sc. Paris, **290 B**, 481–484, 1980.
19. R. HILL and J.R. RICE, *Constitutive analysis of elastic-plastic crystals at arbitrary strain*, J. Mech. Phys. Solids, **20**, 401–413, 1972.
20. H. PETRYK, *On constitutive inequalities and bifurcation in elastic-plastic solids with a yield-surface vertex*, J. Mech. Phys. Solids, **37**, 265–291, 1989.
21. C. STOLZ, *On relationship between micro and macro scales for particular cases of nonlinear behaviour of heterogeneous media*, 617–628, [in]: Proc. of IUTAM/ICM Symposium on Yielding, Damage and Failure of Anisotropic Solids, J.-P. BOEHLER [Ed.], Mechanical Engineering Publications, London 1990.
22. R. HILL, *The essential structure of constitutive laws for metal composites and polycrystals*, J. Mech. Phys. Solids, **15**, 779–795, 1967.
23. D.R. SMITH, *An introduction to continuum mechanics*, Kluwer Academic Publishers, Dordrecht 1993.
24. J. MANDEL, *Thermodynamics and plasticity*, [in]: Foundations of Continuum Thermodynamics, 283–304, J.J. DELGADO DOMINGOS et al. [Eds.], McMillan, London 1974.
25. M. KLEIBER and B. RANIECKI, *Elastic-plastic materials at finite strains*, [in]: Plasticity Today, Modelling, Methods and Applications, 3–46, A. SAWCZUK and G. BIANCHI [Eds.], Elsevier, London 1985.
26. R.B. PEÇHERSKI, *The plastic spin concept and the theory of finite plastic deformations with induced anisotropy*, Arch. Mech., **40**, 807–818, 1988.
27. B. RANIECKI and Z. MRÓZ, *On the strain-induced anisotropy and texture in rigid-plastic solids*, [in]: Inelastic Solids and Structures. A. Sawczuk Memorial Volume, 13–32, M. KLEIBER and A. KÖNIG [Eds.], Pineridge Press, Swansea 1990.
28. S.C. ŢIGOIU and E. SOÓS, *Elastoviscoplastic models with relaxed configurations and internal state variables*, Appl. Mech. Rev., **43**, 131–151, 1990.
29. J.F. BESSELING and E. VAN DER GIESSEN, *Mathematical modelling of inelastic deformation*, Chapman & Hall, London 1994.
30. E.H. LEE, *Elastic-plastic deformation at finite strains*, J. Appl. Mech., **36**, 1–6, 1969.

31. A. KORBEL, *The real nature of shear bands – plastons?*, 325–335, [in:] *Plastic Instability*, Proc. Int. Symp. on Plastic Instability. Considère Memorial (1841–1914), Presses de l'École Nationale des Ponts et Chaussées, Paris 1985.
32. A. PAWEŁEK and A. KORBEL, *Soliton-like behaviour of a moving dislocation group*, *Phil. Mag.*, **61 B**, 829–842, 1990.
33. J.J. GILMAN, *Physical nature of plastic flow and fracture*, 43–99, [in:] *Plasticity*, Proc. of the Second Symp. on Naval Structural Mechanics, E.H. LEE and P.S. SYMONDS [Eds.], Pergamon Press, 1960.
34. G.E. DIETER, *Mechanical metallurgy*, SI Metric Edition — adapted by D. BACON, McGraw-Hill, London 1988.
35. A. KORBEL, *The analyses of the nonuniform deformation in the substitutional solid solutions* [in Polish], *Metalurgia i Odlewnictwo*, **Z. 65**, Zesz. Nauk. AGH, Kraków 1974.
36. M. ZHOU, A.J. ROSAKIS and G. RAVICHANDRAN, *Dynamically propagating shear bands in impact loaded prenotched plates. I. Experimental investigations of temperature signatures and propagation speed*, *J. Mech. Phys. Solids*, **44**, 981–1006, 1996.
37. S. YANG and C. REY, *Shear band postbifurcation in oriented copper single crystals*, *Acta Metall.*, **42**, 2763–2774, 1994.
38. C. REY, P. VIARIS DE LESEGO and R. CHIRON, *Etude de la localisation de la déformation plastique en bandes de cisaillement dans des monocristaux de fer déformés en traction simple*, Proc. 6^{ème} Colloque Franco-Polonais, Hétérogénéités de déformation plastique: aspects microscopiques et macroscopiques, 13, 14 et 15 Novembre 1995, Ecole des Mines de Saint-Etienne [to appear].
39. C. TRUESDELL and R.A. TOUPIN, *The classical field theories*, *Encyclopaedia of Physics*, III/1, S. FLÜGGE [Ed.], Springer-Verlag, Berlin 1960.
40. A.C. ERINGEN and E.S. SUHUBI, *Elastodynamics*, Vol I. *Finite Motions*, Academic Press, New York 1974.
41. W. KOSIŃSKI, *Field singularities and wave analysis in continuum mechanics*, PWN, Warszawa and Ellis Horwood, Chichester 1986.
42. A.C. ERINGEN, *Mechanics of continua*, J. Wiley, New York 1967.
43. S. NEMAT-NASSER and M. HORI, *Micromechanics: Overall properties of heterogeneous materials*, North-Holland, Amsterdam 1993.
44. C. TRUESDELL and W. NOLL, *The non-linear field theories of mechanics*, *Encyclopaedia of Physics*, III/3, S. FLÜGGE [Ed.], Springer-Verlag, Berlin 1965.
45. R.B. PEÇHERSKI, *Model of shear banding based on the idea of potential surfaces forming a vertex on the extremal surface*, *ZAMM*, **74**, 190–192, 1994.
46. R.B. PEÇHERSKI, *Model of plastic flow accounting for the effects of shear banding and kinematic hardening*, *ZAMM*, **75**, 203–204, 1995.
47. R.B. PEÇHERSKI, *Macroscopic effects of micro-shear banding in plasticity of metals* [submitted for publication].
48. B. RANIECKI and H. TANAKA, *On the thermodynamic driving force for coherent phase transformations*, *Int. J. Engng. Sci.*, **32**, 1845–1858, 1994.

INSTITUTE OF FUNDAMENTAL TECHNOLOGICAL RESEARCH
POLISH ACADEMY OF SCIENCES
e-mail: rpecher@ippt.gov.pl

Received October 1, 1996.